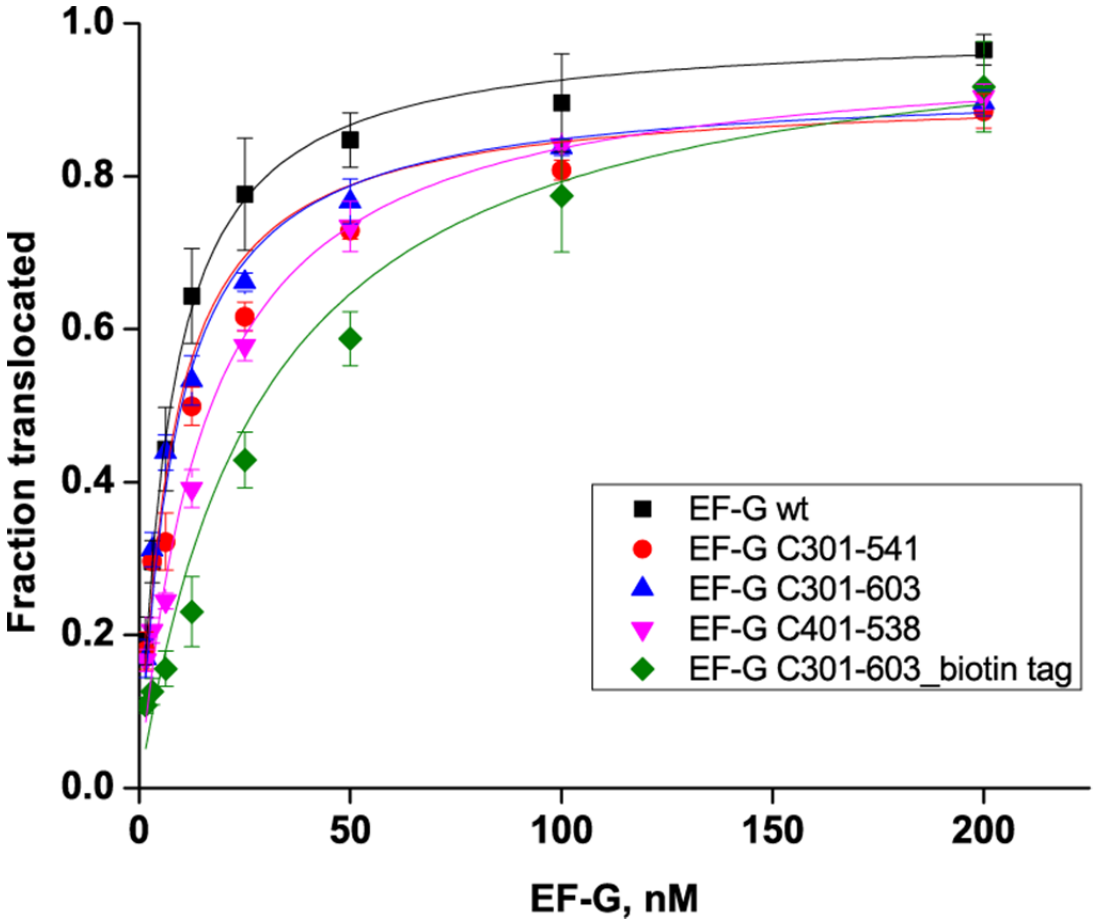

SUPPLEMENTAL FIGURE S1. Activity of doubly-labeled EF-G constructs in multiple turnover translocation. The fraction of translocated ribosomes as a function of EF-G concentration was measured by puromycin reactivity of ribosome-bound tRNA. Translocation in the presence of wild type EF-G (black), EF-G_301-541(Cy3/Cy5) (red), EF-G_301-603(Cy3/Cy5) (blue), EF-G_401-538(Cy3/Cy5) (magenta), and EF-G_301-603(Cy3/Cy5)_biotin tag (green) was carried out in the presence of GTP (0.5 mM) for 2 minutes at 37 ^{o}C. Ribosome concentration was 200 nM. $K_{1/2}$ values, which were determined by fitting the data to hyperbolas, are shown as the respective colored lines, and are reposted in Supplemental Table S2. Error bars show standard deviations calculated from triplicate measurements.

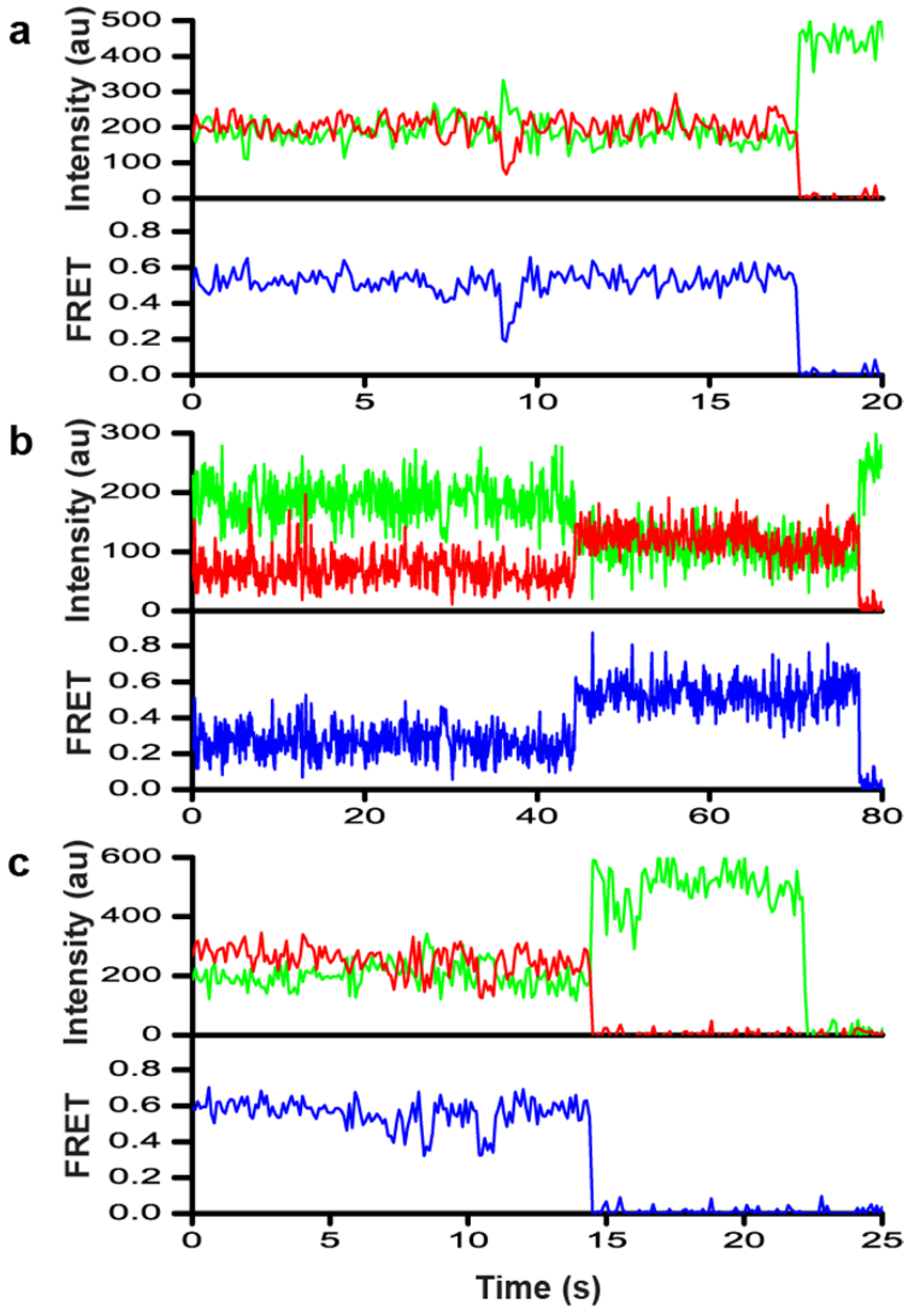

SUPPLEMENTAL FIGURE S2. smFRET traces for EF-G_301-603(Cy3/Cy5)_biotin imaged in the absence of nucleotides (a), presence of GDP (b) and GTP (c). The traces show fluorescence intensities observed for Cy3 (green) and Cy5 (red) and the calculated apparent FRET efficiency (blue). Traces display a predominant 0.6 FRET state with sampling of a lower (~0.3) FRET state.

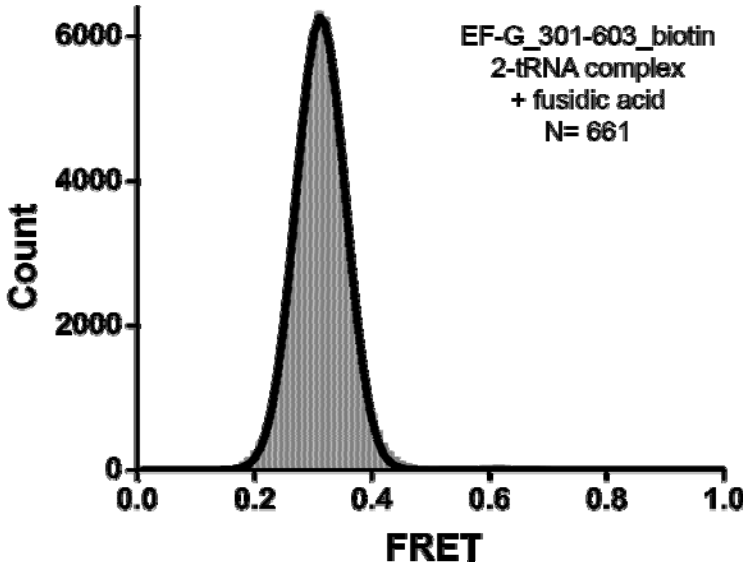

SUPPLEMENTAL FIGURE S3. **Histogram showing distribution of FRET values for biotin-tagged EF-G bound to the posttranslocation ribosome.** EF-G_301-603(Cy3/Cy5)_biotin was incubated with pretranslocation ribosomes containing $tRNA^{Met}$ in the P site and *N*-acetyl-Met-Phe-$tRNA^{Phe}$ in the A site in the presence of GTP and fusidic acid. In order to prevent direct binding of EF-G to the slide surface, 200 μM biotin was added to the sample chamber to saturate the unoccupied biotin binding sites in neutravidin. N is the number of single-molecule traces compiled. The black line shows Gaussian fit.

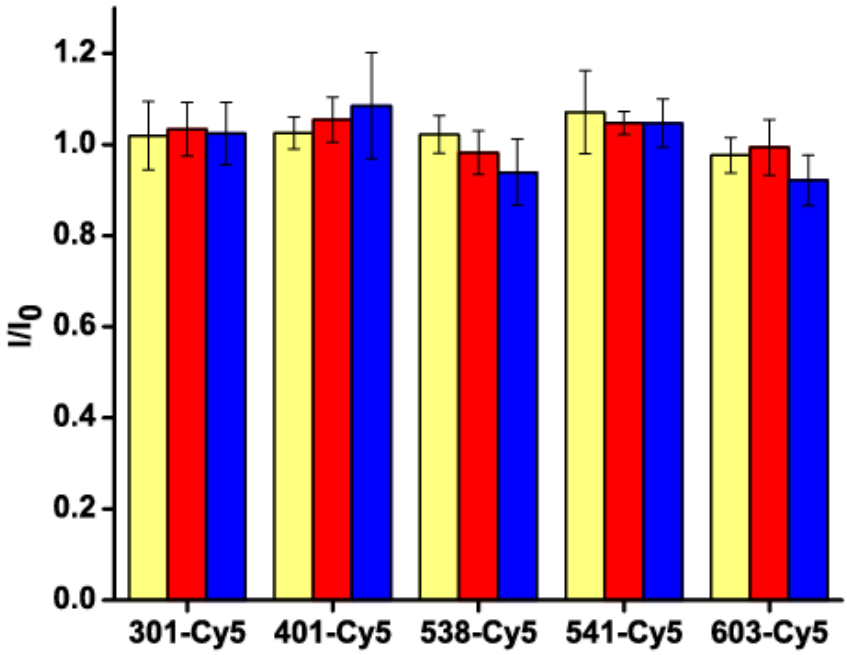

SUPPLEMENTAL FIGURE S4. **Binding of EF-G to the pretranslocation ribosome does not significantly change quantum yield of Cy5 at all positions used for labeling in this work.** Fluorescence emission intensity of Cy5 attached to different labeling sites of EF-G in the presence of 0.5 mM GTP and 40 □M fusidic acid (yellow bars); in EF-G•GTP•fusidic acid incubated with ribosomes containing $tRNA^{Met}$ in the P site in the presence of viomycin (red bars); in EF-G•GTP•fusidic acid incubated with ribosomes containing $tRNA^{Met}$ in the P site and *N*-acetyl-Met-Phe-$tRNA^{Phe}$ in the A site, in the presence of viomycin (blue bars). Intensity of Cy5 fluorescence in each complex (I) was normalized by the fluorescence intensity of Cy5-labeled ribosome-free EF-G (I_0). Error bars show standard deviations calculated from triplicate measurements.

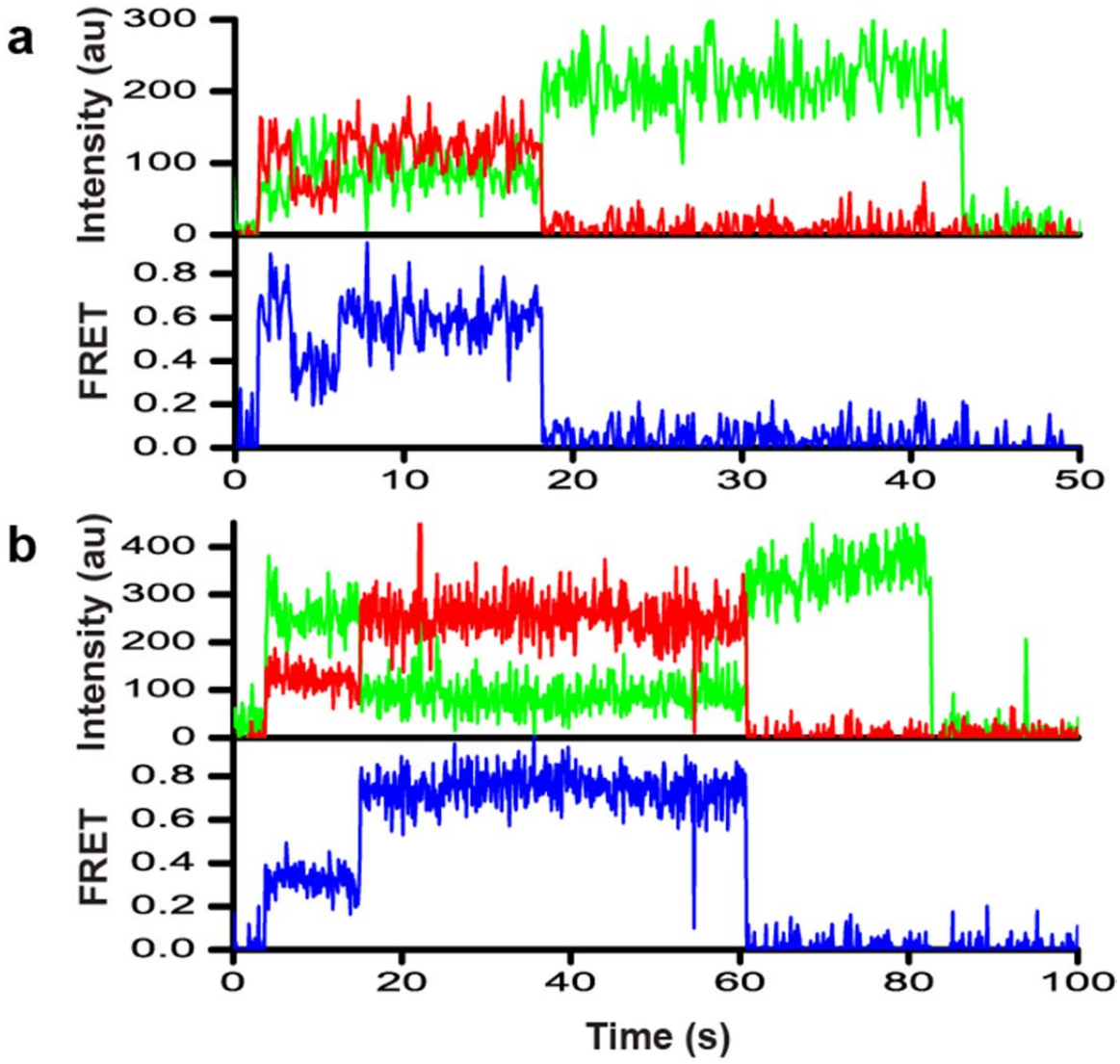

SUPPLEMENTAL FIGURE 5. smFRET traces for posttranslocation EF-G-ribosome complex displaying sampling of the higher (~0.5-0.7) FRET states in addition to the predominant 0.3 FRET state (a-b). EF-G_301-603(Cy3/Cy5) was incubated with pretranslocation ribosomes containing $tRNA^{Met}$ in the P site and *N*-acetyl-Met-Phe-$tRNA^{Phe}$ in the A site in the presence of GTP and fusidic acid. The traces show fluorescence intensities observed for Cy3 (green) and Cy5 (red) and the calculated apparent FRET efficiency (blue).

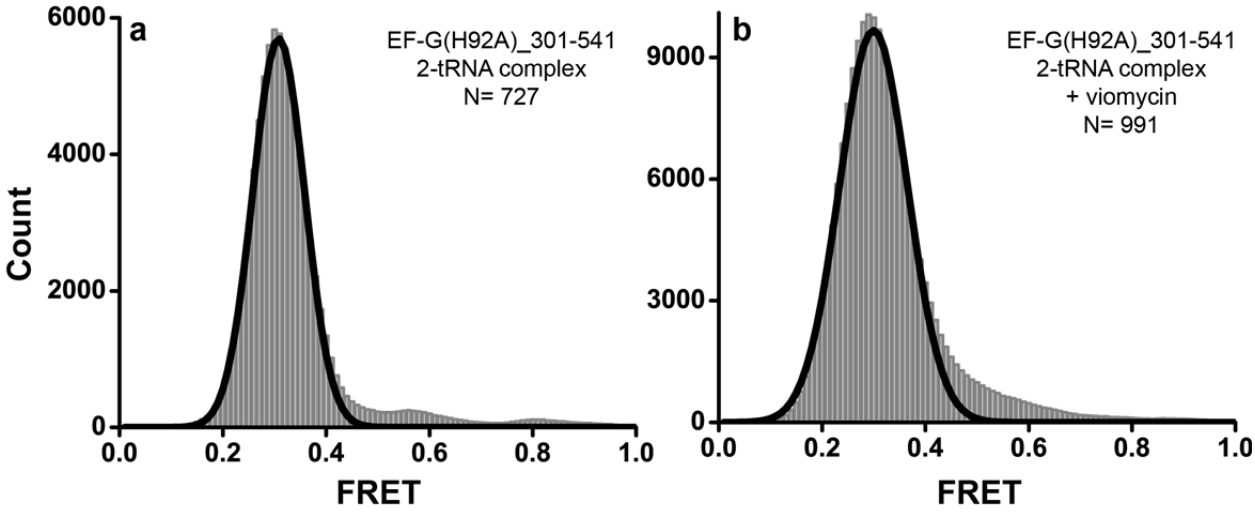

SUPPLEMENTAL FIGURE S6. **Histograms showing distribution of FRET values for EF-G carrying the H92A mutation bound to the pre- and posttranslocation ribosome.** EF-G(H92A)_301-541(Cy3/Cy5) was incubated with pretranslocation ribosomes containing $tRNA^{Met}$ in the P site and *N*-acetyl-Met-Phe-$tRNA^{Phe}$ in the A site in the presence of GTP and absence (a) or presence of viomycin (b). N is the number of single-molecule traces compiled for each histogram. The black line shows Gaussian fit.

SUPPLEMENTAL TABLE S1. Fluorescent labeling and biotin-tagging does not affect translocation activity of EF-G under pre-steady-state conditions.

EF-G variant	k_1, s^{-1}	k_2, s^{-1}	$A_1/(A_1+A_2)$	k_{av}, s^{-1}
wt	5.4±0.9	0.7±0.1	0.49±0.03	3.0±0.5
EF-G_301(Cy5)	7.0±1.7	0.6±0.1	0.36±0.02	2.9±0.7
EF-G_401(Cy5)	3.9±0.5	0.6±0.1	0.42±0.03	2.0±0.2
EF-G_538(Cy5)	7.1±3.0	0.7±0.1	0.40±0.02	3.3±1.3
EF-G_541(Cy5)	5.4±1.6	0.7±0.1	0.34±0.04	2.3±0.7
EF-G_603(Cy5)	4.0±0.5	0.7±0.1	0.41±0.02	2.0±0.2
EF-G_301-603_biotin	3.2±0.8	0.6±0.1	0.32±0.02	1.4±0.2

Rates of translocation catalyzed by Cy5-labeled mutant variants of EF-G were measured in pre-steady-state stopped-flow kinetic experiments as described in the Supplemental Methods. EF-G and ribosome concentrations after mixing were 0.5 μM and 35 nM, respectively. k_1 and k_2 are the rate constants of double-exponential fits of the mRNA translocation data; $A_1/(A_1+A_2)$ is the relative contribution of the faster phase to the total amplitude of fluorescein quenching. Weighted average values (k_{av})[1] for mRNA translocation rates were calculated by combining the rate constants derived from the two-exponential fits: $k_{av} = (k_1A_1 + k_2A_2)/(A_1 + A_2)$.

SUPPLEMENTAL TABLE S2. Translocation activity of EF-G constructs under multiple-turnover conditions.

EF-G variant	$K_{1/2}$, nM
WT	7.3±0.6
EF-G_301-541(Cy3/Cy5)	7.7±0.9
EF-G_301-603-(Cy3/Cy5)	8.4±0.6
EF-G_401-538(Cy3/Cy5)	16.0±1.2
EF-G 301-603(Cy3/Cy5)_biotin	29±4.8

$K_{1/2}$ for multiple turnover translocation catalyzed by wild type EF-G and doubly-labeled EF-G constructs were determined by fitting the data in Supplemental Fig. S1 to hyperbolas.

SUPPLEMENTAL TABLE S3. Comparison of distances derived from smFRET data and known EF-G structures

FRET pair used	Distance between fluorophores or α-carbon atoms of respective amino acid residues (Å)										
	EF-G_{free}			**EF-G_{free} ●GTP**		**EF-G_{free} ●GDP**		**RS_{POST}/EF-G ●GDP●Fus**		**RS_{PRE}/EF-G ●GDP●Vio**	
	FRET	1elo	2xex	FRET	-	FRET	1dar	FRET	2wri	FRET	3j5x
EFG_301/603	53	50	41	53	-	54	50	63	61	63	62
EFG_301/541	-	49	37	-	-	-	50	60	63	60	64
EFG_401/538	-	52	39	-	-	-	54	62	66	62	66

R (FRET) values are distances calculated from apparent FRET efficiencies measured for doubly-labeled (Cy3/Cy5) EF-G constructs using formula $R = R_0\left(\frac{1}{E} - 1\right)^{1/6}$, with R_0 assumed to be equal to 56 Å^2. These calculations are also based on assumptions that apparent FRET is equal to actual FRET efficiency and that the orientation factor κ^2, which affects the R_0 value [*], is equal to ~2/3 [3; 4]. Thus, FRET-derived distances are approximate values of actual distances. FRET-derived distances are compared to distances in between the α-carbon atoms of respective amino acid residues in structures of ligand-free EF-G from *T. thermophilus* (1elo[5]), ligand-free EF-G from *S. aureus* (2xex[6]), EF-G•GDP from T. thermophilus (1dar[5]), EF-G•GDP•Fus bound to a posttranslocation ribosome from *T. thermophilus* (2wri[7]) and EF-G•GDP•viomycin bound to a pretranslocation ribosome from *E.coli* (3j5x[8]) . The identity of each structure is indicated by its respective PDB code.

[*] $R_0 = 0.211(\kappa^2 n^{-4} Q_D J(\lambda))^{1/6}$ where κ^2 is orientation factor; n is the refractive index of the medium, Q_D is the quantum yield of donor in the absence of acceptor, J(λ) is the integral of spectral overlap between the donor emission and acceptor excitation.

SUPPLEMENTAL METHODS

Stopped-flow measurements of pre-steady-state translocation kinetics

The kinetics of mRNA translocation were measured as previously described with minor modifications [1; 9; 10]. Pretranslocation complexes were constructed by the incubation of 70S ribosomes (1 μM) with fluorescein-labeled mRNA (5'-GGC AAG GAG GUA AAA AUG UUU AAA-3'- fluorescein, synthesized by Dharmacon RNAi Technologies, 0.85 μM) and deacylated $tRNA^{Met}$ (2 μM) in polyamine buffer (30 mM HEPES·KOH, pH 7.6, 150 mM NH_4Cl, 6 mM $MgCl_2$, 2 mM spermidine, 0.1 mM spermine, 6 mM β–mercaptoethanol) for 20 minutes at 37 ^oC, followed by an incubation with *N*-acetyl-Phe-$tRNA^{Phe}$ (1.5 μM) for 30 minutes at 37 ^oC. Pretranslocation ribosomes were mixed with wild-type or Cy5-labeled EF-G variants and GTP using an Applied Photophysics stopped-flow fluorometer. Final concentrations after mixing were: 35 nM ribosomes, 0.5 μM EF-G and 0.5 mM GTP. Fluorescein was excited at 480 nm and fluorescence emission was detected using a 515 nm long-pass filter. All stopped-flow experiments were done at 23 ^oC; monochromator slits were adjusted to 9.3 nm. Translocation of mRNA resulted in partial quenching of fluorescein coupled to the 3' end of the mRNA [9]. Time traces were analyzed using Pro-Data-Viewer software (Applied Photophysics). As reported previously [1; 11; 12], the kinetics of mRNA translocation are clearly biphasic and are best fitted to the sum of two exponentials, corresponding to the apparent rate constants k_1 and k_2. Although the biphasic character of fluorescence changes associated with mRNA translocation is well documented, the physical basis of this phenomenon remains unclear. The rate of translocation was defined as the weighted average rate constant k_{av} (Supplemental Table S1), calculated as the

sum of k_1 and k_2 normalized to their respective contributions to the total amplitude of fluorescence change [$k_{av} = (k_1A_1 + k_2A_2)/(A_1 + A_2)$] [1].

Multiple-turnover translocation assay

Translocation activity of doubly-labeled EF-G constructs was measured by puromycin reactivity of ribosome-bound tRNA (Supplemental Fig. S1 and Supplemental Table S2)[13]. Pretranslocation ribosome complexes were assembled using 70S ribosomes (0.2 μM) incubated with mRNA m32 (0.4 μM) and deacylated $tRNA^{fMet}$ (0.4 μM) in polyamine buffer (see above) for 20 min at 37 °C. Radiolabeled *N*-acetyl-[^{3}H]Phe-$tRNA^{Phe}$ (0.35 μM) was subsequently added to the mixture and incubated for another 20 min at 37 °C. Translocation was catalyzed by the addition of GTP (0.5 mM) and EF-G at concentrations varying between 1 and 200 nM, followed by incubation for 2 min at 37 °C, *i.e.* under initial velocity conditions for 1-10 nM EF-G. Puromycin (1 mM) was then added and incubated for 3 min at 37 °C. The *N*-acetyl-[^{3}H]Phe•puromycin products were separated from the reaction mixture by the addition of 70 μL extraction buffer ($MgSO_4$-saturated 0.3 M NaOAc, pH 5.3) to a final reaction volume of 80 μL, and then 1 mL ethyl acetate was added. The ethyl acetate fraction was separated from the aqueous phase by centrifugation and incubated with scintillation fluid, followed by the measurement of radioactivity.

Ensemble fluorescence measurements

Ensemble fluorescence measurements were taken using a FluoroMax-4 spectrofluorometer (Horiba) at 22°C. A sample volume of 30 μl was used to overfill the clear window of the 10 μl cuvette (Starna Cells). For the checking of changes in Cy5 quantum yield (Supplemental Fig. S4), Cy5 emission spectra were taken by exciting fluorescence at 635 nm (emission 645-800 nm) in single-labeled EF-G constructs. The slit-widths for both excitation and emission were set to 5

nm of spectral band-width. All reactions and EF-G complexes were assembled in polyamine buffer containing 20 mM Hepes-KOH, pH 7.5, 6 mM $MgCl_2$, 150 mM NH_4Cl, 6 mM β-mercaptoethanol, 2 mM spermidine, 0.1 mM spermine and 0.01% Nikkol. The pretranslocation ribosomes containing *N*-acetyl-Met-Phe $tRNA^{Phe}$ in the A site and $tRNA^{Met}$ in the P site were assembled as described in **Materials and Methods** of the main manuscript. The concentration of Cy5-labeled EF-G was 100 nM, 70S ribosome was 200 nM, GTP was 0.5 mM, fusidic acid was 40 μM, and viomycin was 0.5 mM.

References:

1. Ermolenko, D. N. & Noller, H. F. (2011). mRNA translocation occurs during the second step of ribosomal intersubunit rotation. Nat Struct Mol Biol 18, 457-62.
2. Dietrich, A., Buschmann, V., Muller, C. & Sauer, M. (2002). Fluorescence resonance energy transfer (FRET) and competing processes in donor-acceptor substituted DNA strands: a comparative study of ensemble and single-molecule data. J Biotechnol 82, 211-31.
3. Roy, R., Hohng, S. & Ha, T. (2008). A practical guide to single-molecule FRET. Nat Methods 5, 507-16.
4. Clegg, R. M. (1992). Fluorescence resonance energy transfer and nucleic acids. Methods Enzymol 211, 353-88.
5. AEvarsson, A., Brazhnikov, E., Garber, M., Zheltonosova, J., Chirgadze, Y., al-Karadaghi, S., Svensson, L. A. & Liljas, A. (1994). Three-dimensional structure of the ribosomal translocase: elongation factor G from Thermus thermophilus. EMBO J 13, 3669-77.
6. Chen, Y., Koripella, R. K., Sanyal, S. & Selmer, M. (2010). Staphylococcus aureus elongation factor G--structure and analysis of a target for fusidic acid. FEBS J 277, 3789-803.
7. Gao, Y. G., Selmer, M., Dunham, C. M., Weixlbaumer, A., Kelley, A. C. & Ramakrishnan, V. (2009). The structure of the ribosome with elongation factor G trapped in the posttranslocational state. Science 326, 694-9.
8. Brilot, A. F., Korostelev, A. A., Ermolenko, D. N. & Grigorieff, N. (2013). Structure of the ribosome with elongation factor G trapped in the pretranslocation state. Proc Natl Acad Sci U S A 110, 20994-9.
9. Studer, S. M., Feinberg, J. S. & Joseph, S. (2003). Rapid kinetic analysis of EF-G-dependent mRNA translocation in the ribosome. J Mol Biol 327, 369-81.
10. Svidritskiy, E., Ling, C., Ermolenko, D. N. & Korostelev, A. A. (2013). Blasticidin S inhibits translation by trapping deformed tRNA on the ribosome. Proc Natl Acad Sci U S A 110, 12283-8.

11. Peske, F., Savelsbergh, A., Katunin, V. I., Rodnina, M. V. & Wintermeyer, W. (2004). Conformational changes of the small ribosomal subunit during elongation factor G-dependent tRNA-mRNA translocation. J Mol Biol 343, 1183-94.
12. Munro, J. B., Altman, R. B., Tung, C. S., Cate, J. H., Sanbonmatsu, K. Y. & Blanchard, S. C. (2010). Spontaneous formation of the unlocked state of the ribosome is a multistep process. Proc Natl Acad Sci U S A 107, 709-14.
13. Salsi, E., Farah, E., Dann, J. & Ermolenko, D. N. (2014). Following movement of domain IV of elongation factor G during ribosomal translocation. Proc Natl Acad Sci U S A, 10.1073/pnas.1410873111.